Cardiovascular Research (2013) **98**, 504–514
doi:10.1093/cvr/cvt076

# Functional suppression of Kcnq1 leads to early sodium channel remodelling and cardiac conduction system dysmorphogenesis

**Angel J. de la Rosa[1,2,3], Jorge N. Domínguez[1,2,3], David Sedmera[4], Bara Sankova[2,3], Leif Hove-Madsen[2,3], Diego Franco[1,2,3], and Amelia E. Aránega[1,2,3]***

[1]Department of Experimental Biology, Faculty of Experimental Sciences, University of Jaén, Paraje de las Lagunillas, s/n, Jaén 23071, Spain; [2]Department of Cardiovascular Morphogenesis, Institute of Physiology, Academy of Sciences of the Czech Republic, Prague, Czech Republic; [3]Cardiovascular Research Center CSIC-ICCC, Hospital de la Santa Creu i Sant Pau, Barcelona, Spain; and [4]First Faculty of Medicine, Institute of Anatomy, Charles University, Prague 12800, Czech Republic

*Received 25 August 2012; revised 12 March 2013; accepted 20 March 2013; online publish-ahead-of-print 29 March 2013*

**Time for primary review: 27 days**

**Aims** Ion channel remodelling and ventricular conduction system (VCS) alterations play relevant roles in the generation of cardiac arrhythmias, but the interaction between ion channel remodelling and cardiac conduction system dysfunctions in an arrhythmogenic context remain unexplored.

**Methods and results** We have used a transgenic mouse line previously characterized as an animal model of Long QT Syndrome (LQTS) to analyse ion channel remodelling and VCS configuration. Reverse transcriptase-PCR and immunohistochemistry analysis showed early cardiac sodium channel upregulation at embryonic stages prior to the onset of Kv potassium channel remodelling, and cardiac hypertrophy at foetal stages. In line with these findings, patch-clamp assays demonstrated changes in sodium current density and a slowing of recovery from inactivation. Functional analysis by optical mapping revealed an immature ventricular activation pattern as well as an increase in the total left ventricle activation time in foetal transgenic hearts. Morphological analysis of LQTS transgenic mice in a $Cx40^{GFP/+}$ background demonstrated VCS dysmorphogenesis during heart development.

**Conclusions** Our data demonstrate early sodium channel remodelling secondary to $I_{Ks}$ blockage in a mouse model of LQTS leading to morphological and functional anomalies in the developing VCS and cardiac hypertrophy. These results provide new insights into the mechanisms underlying foetal and neonatal cardiac electrophysiological disorders, which might help understand how molecular, functional, and morphological alterations are linked to clinical pathologies such as cardiac congenital anomalies, arrhythmias, and perinatal sudden death.

**Keywords** Ion channels • Long-QT syndrome • Sudden death • Cardiac hypertrophy

## 1. Introduction

Membrane ion channels and transporters are key determinants of cardiac electrical function. Specialized cardiac electrical properties are determined by characteristic expression profiles of cardiac ion channels. This is critical for a range of physiological processes including action potential (AP) generation and propagation. Cardiac disease importantly alters ion channel expression in ways that promote arrhythmogenesis and contractile dysfunction.[1] Abnormalities in cardiac ion channel function or in their associated regulatory proteins may lead to arrhythmias and sudden cardiac death. Therefore, mutations involving cardiac ion channels result in abnormal AP formation or propagation, leading to cardiac arrhythmias classified as cardiac channelopathies such as congenital long QT syndrome (LQTS), Brugada syndrome, catecholaminergic polymorphic ventricular tachycardia, and short-QT syndrome.[1]

In addition to ion channel defects, alterations in the cardiac conduction system (CCS) especially the His-Purkinje system have also been implicated as an important factor in lethal ventricular arrhythmias, such as ventricular fibrillation and drug-induced *torsades des pointes*.[2] In the CCS, ion channels are specialized and differ from those in the working myocardium, as they provide the electrical activity

* Corresponding author. Tel: +34 953 212604; fax: +34 953 211875, Email: aaranega@ujaen.es

required for its proper function. Although changes in the expression and/or configuration of ion channels and connections within the conduction system may have fatal consequences—they can generate arrhythmogenic processes—, the role of the His-Purkinje system in the genesis and maintenance of ventricular arrhythmias secondary to LQTS are not yet well understood.

In this study, we compared changes in ion channel expression and ventricular conduction system (VCS) configuration in the transgenic model of LQTS generated by Demolombe *et al.*[3] In this model, KvLQT1 (Kcnq1) was functionally invalidated by overexpression of the dominant-negative isoform-2 under the control of the α-myosin heavy chain promoter. We observed that these mice developed cardiac hypertrophy at foetal stages. Optical mapping analyses revealed that transgenic embryonic and foetal hearts also presented aberrant VCS function, which correlated with the abnormal architecture detected by morphological examination. Moreover, we found that remodelling of cardiac sodium channel was already present at embryonic stages in these transgenic mice. These observations indicate that sodium channel remodelling and VCS alterations occur very early during heart development, prior to Kv potassium channel remodelling and before the onset of the cardiac hypertrophy in this transgenic model of LQTS. In addition, this finding suggests that ion channel remodelling and aberrant VCS architecture may be associated with underlying arrhythmogenic pathologies such as LQTS.

# 2. Methods

All the experiments were performed in accordance with the European Commission Directive 86/609/EEC (European Convention for the Protection of Vertebrate Animals used for Experimental and Other Scientific Purposes) and approved by the Animal Use and Care Committee of the University of Jaén.

## 2.1. Embryonic and adult transgenic mice

The transgenic mice overexpressing human KvLQT1 dominant-negative isoform (α-MHC-KvlQT1-iso2-T7)[3] was kindly provided by the group of Denis Escande (Nantes, France). Adult mice (6–8 months) and female pregnant mice were killed by cervical dislocation and adult whole hearts as well as embryonic whole hearts from embryonic day (E) 14.5 and E18.5 were isolated as previously described.[4] Cardiac hypertrophy was determined by heart weight/body weight ratio, myocardial cross-sections, and expression levels of two cardiac hypertrophy markers, α-smooth muscle actin (α-SMA) and β myosin heavy chain (β-MHC) in adult, foetal (E18.5) and embryonic (E14.5) hearts. Nav1.5 and Connexin 43 expression were evaluated by immunohistochemistry and western blot. Further details are provided in the Supplemental Material.

## 2.2. Electrocardiogram and patch-clamp recordings

Mice were anaesthetized with 2 mg/kg ketamine (PARKE-DAVIS, S.L.) intraperitoneally as described elsewhere.[5] Electrocardiogram (ECG) recordings were registered and analysed using a digital acquisition and analysis system (Power Lab/4SP; www.adinstrument.com www.adinstrument.com). Adequate anaesthesia was ensured by monitoring heart rate and the absence of a withdrawal response to a paw pinch. When recordings were finished, animals were euthanized by ketamine overdose followed by cervical dislocation. Further details are provided in the Supplemental Material.

Ventricular cardiomyocytes were isolated from adult male mice using a dissociation method similar to that previously described.[6] Briefly, adult male mice were killed by cervical dislocation. The heart was rapidly removed; the aorta was cannulated on a Langendorf system. A calcium containing solution was used to (for 2–3 min) to rinse out remaining blood. Enzymatic digestion was performed as previously described[6] and calcium-tolerant, quiescent, rod-shaped cells with clear, regular cross-striations were selected for electrophysiological recordings. Sodium currents were recorded in the ruptured patch configuration of the patch-clamp technique at room temperature in 14 ventricular myocytes from five H05 hearts and eight myocytes from five WT littermates. Pipette resistances were between 1 and 1.5 Mega-Ohms. Series resistance compensation was used to maximize voltage control. Extracellular solutions contained (in mM): NaCl 11, CsCl 116, $MgCl_2$ 1, $CaCl_2$ 1, HEPES 10, and glucose 10. pH was adjusted to 7.4 with CsOH. The intracellular medium contained (in mM): $CsCl_2$ 146, EGTA 10, $Mg_2ATP$ 3, $MgCl_2$ 1, $Na_2$Phosphocreatine 4, $Li_2GTP$ 0.42, HEPES 10. pH was adjusted to 7.2 with CsOH. The current–voltage relationship was established using 3 mV depolarization steps with a holding potential of −100 mV. The time for recovery from inactivation was determined by stepwise increases (of 2.5 ms) in the interval between two successive 50 ms depolarization from −100 to −40 mV.

## 2.3. Quantitative reverse transcriptase-PCR (qRT–PCR) analyses

Tissue sample and RNA isolation were performed using standard procedures. Reverse transcriptase (RT)-PCR was performed in the Mx3005Tm QPCR System with an Mxpro QPCR Software 3000 (Stratagene) and SYBR Green detection System. Detailed information regarding mRNA quantitative (q)RT–PCR analyses is provided in Supplemental Material.

## 2.4. Primary mouse embryonic cardiomyocytes and mouse embryo cultures

A previously described method was modified to isolate and culture embryonic day 14.5 (E14.5) embryonic cardiomyocytes.[7] Briefly, pregnant mice were sacrificed by cervical dislocation. Embryos were excised and transferred to +2°C. Embryonic hearts were microdissected under a stereomicroscope. Dissected embryonic hearts were submitted to mechanical and chemical disaggregation as previously described.[7] Further details are provided in Supplemental Material.

Embryonic cultured cardiomyocytes were treated with Chromanol 293B (10 mM) for 24 h. Chromanol 293B was diluted at the time of use from a 10 mM stock solution containing 100% DMSO. The concentrations of chromanol 293B (10 mM) were comparable to those used by others and shown to block IKs in other species.[8]

For mouse embryo cultures, embryos ranging from 10- to 12-somites (E8.5–E9.5) stages were cultured until + E10.5 stage as described.[9] Three experimental conditions were used. Thus, a group of 15 cultured embryos were treated with Chromanol 293B (10 μM), whereas a second group of 15 embryos was provided with Anemona sulcata toxin (ATXII) (1 μM). As control, 15 cultured embryos were supplied with Chromanol 293B and ATXII solvent. After culture embryos were washed in PBS, cryopreserved in sucrose solutions, included in OCT, frozen, and cryosectioned. Sections were examined with a fluorescence microscope (Zeiss Axiophot II).

## 2.5. Optical mapping

For optical recordings, adult hearts were removed from the chest and immediately perfused through the coronary circulation via the aorta with oxygenated Tyrode solution at 125 mm Hg. Hearts were stained via superfusion and perfusion with voltage-sensitive dye (di-4-ANEPPS) for 10 min, as previously described.[10]

Hearts from embryonic stages (E14.5) and foetal stages (E18.5) were isolated with a piece of torso attached and stained with the voltage-sensitive dye di-4-ANEPPS (0.002% solution in Tyrodes-HEPES buffer,

pH 7.4; Molecular Probes and Sigma, respectively) for 5 min at room temperature. Details about optical mapping technique mice were provided recently[11] and described in Supplemental Material.

### 2.6. Cardiac conduction system analysis

To perform the morphological analysis of the CCS, α-MHC-KvlQT-iso2-T7 mice were crossed with $CX40^{GFP}/+$ mice, kindly provided by Lucile Miquerol (Developmental Biology Institute of Marseilles-Luminy, Marseille, France). Adult, foetal, and embryonic hearts were obtained as previously described.[4] Adult hearts and foetal hearts (E18.5) were examined after dissection for observation by stereomicroscope equipped for GFP detection. Visualization and quantification of Cx40-positive cell networks using fluorescent illumination was performed as described previously.[12] E14.5 and E16.5 hearts were cryopreserved in sucrose solutions, included in OCT, frozen, and cryosectioned. Sections were examined with a fluorescence microscope (Zeiss Axiophot II) and Cx40-positive trabeculations were quantified by using Image J software. Further details are provided in Supplemental Material.

### 2.7. Statistical analyses

Categorical data are described as frequency and percentage. Continuous data are presented as mean ± SD. We used the Chi-square test to test for differences in ventricular activation patterns. Continuous variables were compared using unpaired Student's *t*-test. A *P*-value $<0.05$ was considered statistically significant.

## 3. Results

### 3.1. Sodium channel remodelling and cardiac hypertrophy in the α-MHC-KvLQT1-iso2-T7 transgenic model of LQTS

The α-MHC-KvLQT1-iso2-T7 transgenic mouse model was generated and characterized by Demolombe *et al.*[3] In this mouse model the KvLQT1 $K^+$ channel was functionally inactivated by overexpression of its dominant-negative isoform-2 under the control of alpha-myosin heavy chain promoter. This α-MHC-KvLQT1-iso2-T7 mouse model shares common features with the LQTS in patients including long QT and sinus node dysfunction.[3] Among the three transgenic lines established (H02, H05, H08), H02 and H08—but not H05—lines also displayed atrioventricular block. In this study, we used the H05 transgenic line, which presents a prolonged QT interval as the main electrocardiographic finding (see Supplementary material online, *Figures S1A–B*). Interestingly, H05 mice display a significantly lower survival rate at 1 year of follow-up as well as morphologic and molecular signs of cardiac hypertrophy (see Supplementary material online, *Figure S2A–D*).

LQTS is related to $K^+$ channel mutations and cardiac sodium channel mutations (SCN5A).[1,13] It has been previously described that the α-MHC-KvLQT1-iso2-T7 mouse model displays molecular remodelling of other $K^+$ channels such as the Kv4.2, Kv4.3, and Kv1.5, thus suggesting that this Kv channel remodelling might be responsible for a significant part of the ECG phenotype in these transgenic mice.[3] However, recent studies have revealed that increases in sodium currents ($I_{Na}$) seem to be an important factor in the prolongation of AP duration and the generation of polymorphic ventricular tachycardia in repolarization disorders such as the LQTS.[14] Therefore, to investigate whether there is cardiac sodium channel remodelling in the H05 transgenic line, we analysed by RT–PCR, western blot and immunohistochemistry the expression levels of the Nav1.5 cardiac sodium channel α-subunit (encoding by Scn5a), as well as the expression levels of its main regulatory subunit: the auxiliary β1-subunit (encoding by Scn1b).[15,16] This analysis revealed that Scn5a and Scn1b were clearly increased in H05 α-MHC-KvLQT1-iso2-T7 transgenic mice, when compared with wild-type littermate (*Figure 1A–F*), indicating that this mouse model of LQTS displays a clear cardiac sodium channel upregulation.

### 3.2. Early embryonic sodium channel remodelling precedes the onset of cardiac hypertrophy and is secondary to functional suppression of KvLQT1 channel

To elucidate the timing of the onset of ion channel remodelling and cardiac hypertrophy in α-MHC-KvLQT1-iso2-T7 H05 transgenic mice, we carried out morphological and molecular analyses at two different time points of heart development; (i) embryonic stage (E14.5) when heart septation still is just completed and the ventricular wall is still fairly trabeculated and (ii) foetal stage (E18.5) where a four-chamber heart with fully vascularized ventricular compact layer is formed.[17] We found that increases in sodium channel subunits (i.e. Scn5a and Scn1b) were detected in the hearts of H05 mice as early as at embryonic stages (E14.5) (*Figure 1G–K*) and were maintained at foetal stages (*Figure 1H–N*). Morphological and molecular signs of cardiac hypertrophy, including increases in myocardial cross-section with no differences in cell proliferation as well as molecular remodelling of the potassium channels Kv4.2, Kv4.3, and Kv1.5 were also detected in the H05 hearts at foetal stage (E18.5) but not at embryonic stage (see Supplementary material online, *Figures S3, S4A–F*, and *S5*). In this context, it is interesting to highlight that Scn5a and Scn1b upregulation were not detected in the very early transgenic hearts (E10.5) (see Supplementary material online, *Figure S4G*), thus excluding the possibility that upregulation of sodium channel would be concurrent with the expression of KvlQT1iso2-T7 in the developing heart. Taken together, these results indicate that cardiac sodium channel upregulation in this transgenic model occurs as early as embryonic stages before the onset of cardiac hypertrophy phenotype and potassium channel remodelling at foetal stages. This suggests that functional suppression of the KvLQT1 potassium channel may lead to sodium channel upregulation during development.

Therefore, to further analyse the relationship between potassium channel functional disruption and sodium channel expression at early developmental stages, we performed *in vitro* and *ex vivo* experiments by using primary mouse embryonic cardiomyocyte culture as well as embryo culture in which KvLQT1 (Kcnq1) potassium channels were blocked by Chromanol 293B treatment.[8] In line with our *in vivo* findings, qRT–PCR analysis showed that the expression levels of Scn5a and Scn1b were increased in isolated mouse embryonic cardiomyocytes after 24 h of Chromanol 293B treatment (*Figure 2A*). Similarly, *ex vivo* experiments revealed that Scn5a and Scn1b mRNA transcripts were clearly upregulated in the hearts of the cultured embryos treated 24 h with Chromanol 293B (*Figure 2B*). This indicates that functional disruption of KvLQT1 channels may trigger Scn5a and Scn1b expression in the embryonic heart.

### 3.3. Sodium current recordings in isolated cardiomyocytes from the H05 line of the α-MHC-KvLQT1-iso2-T7 transgenic model

To determine whether sodium channel upregulation detected in the hearts of H05 mice affects sodium current density, patch-clamp

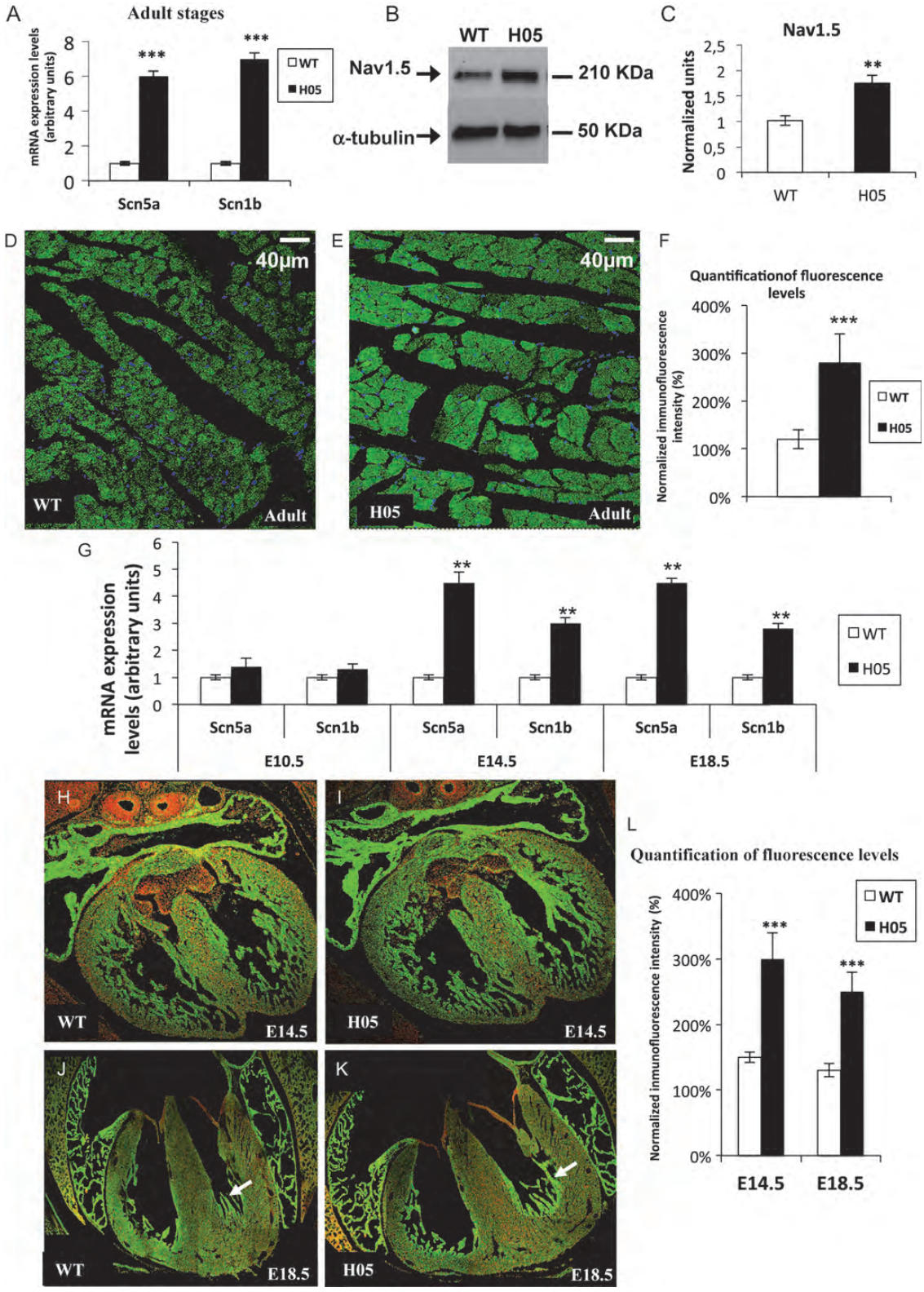


**Figure 1** (*A*) qRT–PCR for Scn5a and Scn1b in adult transgenic and control hearts ($n = 5$). (*B* and *C*) Western blots for Nav1.5 protein ($n = 3$). (*D* and *E*) Immunohistochemistry analysis for Scn5a (Nav1.5). (*G*) qRT–PCR for Scn5a and Scn1b in E10.5, E14.5, E18.5 H05 and control hearts ($n = 5$ per stage). (*H–K*) Immunohistochemistry analyses for Scn5a at E14.5 and E18.5. Although Scn5a expression is higher within the developing ventricular conduction system when compared with working myocardium as previously documented,[4,17] Scn5a expression is enhanced in the embryonic and foetal H05 hearts respect to control (arrows). (*F* and *L*) Semi-quantitative analysis of fluorescence intensity. All measured intensities in one section were performed in at least five different fields and expressed as a percentage of the average intensity value. Results are averaged from measured performed in three hearts and three sections per heart (total number of sections analysed = 9). $^{**}P < 0.001$, $^{***}P < 0.0001$.

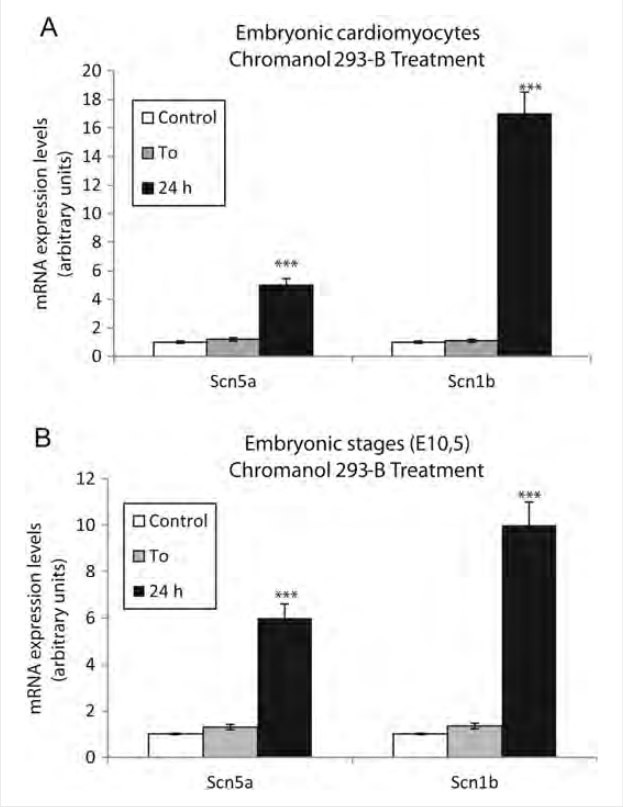


**Figure 2** qRT–PCR for Scn5a and Scn1b in rolling embryonic culture (*A*) and primary cultures of embryonic cardiomyocytes (*B*) treated with chromanol 293-B ($n = 15$). To: Time 0 of treatment. ***$P < 0.0001$.

experiments were performed using isolated ventricular cardiomyocytes of age-and-sex-matched control and transgenic adult mice, respectively. To characterize the sodium current, we focused on four aspects (i) current–voltage relationship, (ii) voltage-dependent inactivation, (iii) inactivation kinetics, and (iv) recovery time from inactivation.

*Figure 3A* shows a representative family of current traces recorded at increasing test potentials; and the current–voltage (I–V) relationship shown in *Figure 3B* demonstrated that peak current densities were 30–40% higher in 14 H05 transgenic ventricular myocytes from five hearts when compared with 8 ventricular myocytes from 5 WT littermates. Similarly, the conductance–voltage relationship shown in Supplementary material online, *Figure S6A* revealed a 30–40% higher conductance in H05 myocytes. Analysis of voltage-dependent inactivation showed no differences between H05 transgenic and WT myocytes when normalized currents were plotted as a function of membrane potentials and fitted by a Boltzmann equation (see Supplementary material online, *Figure S6B*). Moreover, fitting the decay of $I_{Na}$ with a double exponential revealed no differences in fast or slow inactivation of $I_{Na}$ among myocytes from H05 and WT littermates (see Supplementary material online, *Figure S6C*). However, the recovery time from inactivation was slower in H05 transgenic than in WT ventricular myocytes (*Figure 3 C–D*).

Thus, patch-clamp analysis revealed that the functional consequences of cardiac sodium channel upregulation in the H05 line of the α-MHC-KvLQT1-iso2-T7 transgenic model includes an increase in the peak sodium current density and a slowed recovery from inactivation.

## 3.4. Functional analysis by ventricular optical mapping

In the present work, we found Scn5a and Scn1b up-regulation in the hearts of H05 transgenic line as early as at the embryonic stages of development (E14.5). Previous results obtained at our laboratory pointed out that Scn5a and Scn1b genes are significantly enhanced in the VCS during mouse cardiogenesis, indicating that they might play an important role in the development of the mature ventricular activation pattern.[4,16] It has been previously shown that changes in ventricular activation patterns correlate with CCS development and maturation.[11,18] Therefore, optical mapping analysis was performed at the embryonic (E14.5) and foetal stages (E18.5) to determine whether sodium channel upregulation in H05 transgenic hearts has functional effects on the development of the mature ventricular activation pattern. This analysis showed that embryonic WT hearts mainly present a left–right ventricular activation pattern (60%), whereas embryonic H05 hearts mostly display a left ventricular activation pattern (64%), indicating a perturbed function of the developing right bundle branch (*Figure 4A–E*). Similarly, foetal WT ventricles have a predominant left–right activation pattern (94%) while foetal H05 hearts maintain a marked left ventricular activation pattern (84%) (*Figure 4F–J*). These results demonstrate that H05 hearts display an abnormal ventricular activation pattern during development.

In addition, we analysed the total left ventricular activation time under two different experimental conditions: (i) spontaneous beating, where the electrical impulse is transmitted through the VCS, and (ii) electrically stimulated contraction where the heart is stimulated by an electrode and the electrical impulse is transmitted solely through the working myocardium.[18] We found that under spontaneous rhythm, the total left ventricular activation time was similar in H05 transgenic and wild-type hearts at the embryonic stages (E.14.5) (*Figure 4L*), but an increase in the total left ventricular activation time was detected in H05 transgenic hearts, when compared with WT littermates at the foetal (E18.5) and adult stages (*Figure 4K–N*). Furthermore, analyses of total left ventricular activation time under stimulated contraction revealed no differences between H05 hearts and wild-type littermates at any stage (*Figure 4L–N*), indicating that electrical impulse transmission through the working myocardium is not altered in H05 transgenic hearts. Since working myocardium cardiomyocytes are linked together by Cx43 clusters forming gap junctions,[19] we also analysed Cx43 expression levels and protein distribution in adult hearts of the H05 transgenic line. Our results show that both Cx43 expression levels and protein distribution were comparable between transgenic animals and WT littermates (see Supplementary material online, *Figure S7*) in line with the normal impulse propagation through the working myocardium discovered by optical mapping (*Figure 4K*). These findings indicate that foetal and adult H05 ventricles present a delay in the transmission of the electrical impulse, most likely due to impaired CCS function.

## 3.5. Morphological anomalies in the VCS of the H05 line of α-MHC-KvLQT1-iso2-T7 transgenic mice

Since optical mapping of H05 mice hearts showed a delay in the acquisition of a mature ventricular activation pattern during development and functional alterations were found in the impulse propagation through the VCS, we next analysed the architecture of

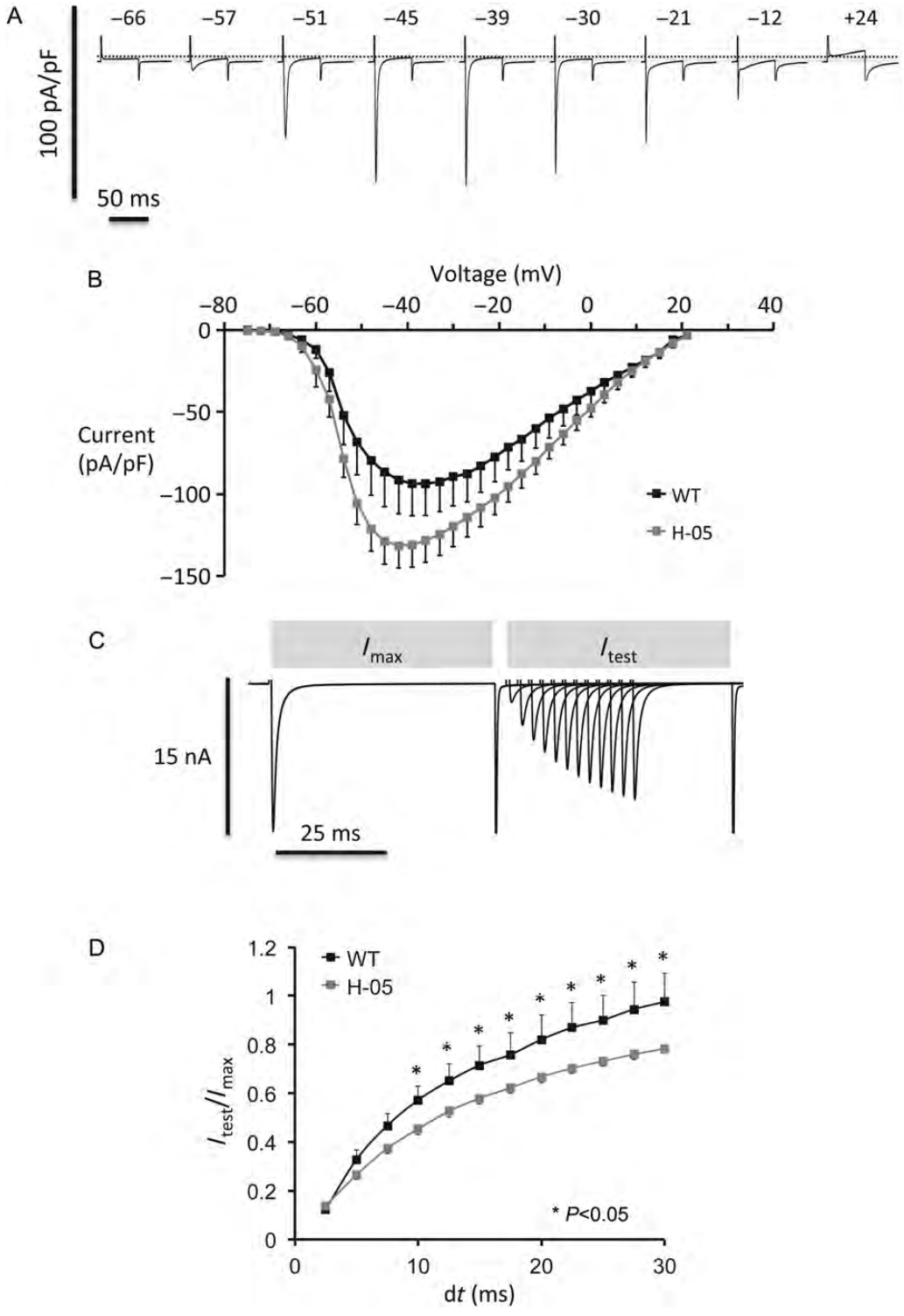


**Figure 3** Patch-clamp analyses: (*A*) representative current traces recorded in a WT ventricular myocyte. The holding potential was -100 mV and test potentials are given above each trace. Horizontal scale bar is 50 ms and vertical scale bar is 100 pA/pF. (*B*) Current–voltage (I–V) relationship for the sodium current recorded in 14 isolated adult transgenic H05 and 8 WT ventricular myocytes. (*C*) Family of sodium currents recorded with increasing intervals (dt) between two consecutive depolarization pulses ($I_{max}$ and $I_{test}$). (*D*) Recovery of the sodium current from inactivation in isolated adult transgenic H05 and WT ventricular myocytes. Values shown are $I_{test}/I_{max}$. * Indicates a significant difference between the H05 and WT myocytes.

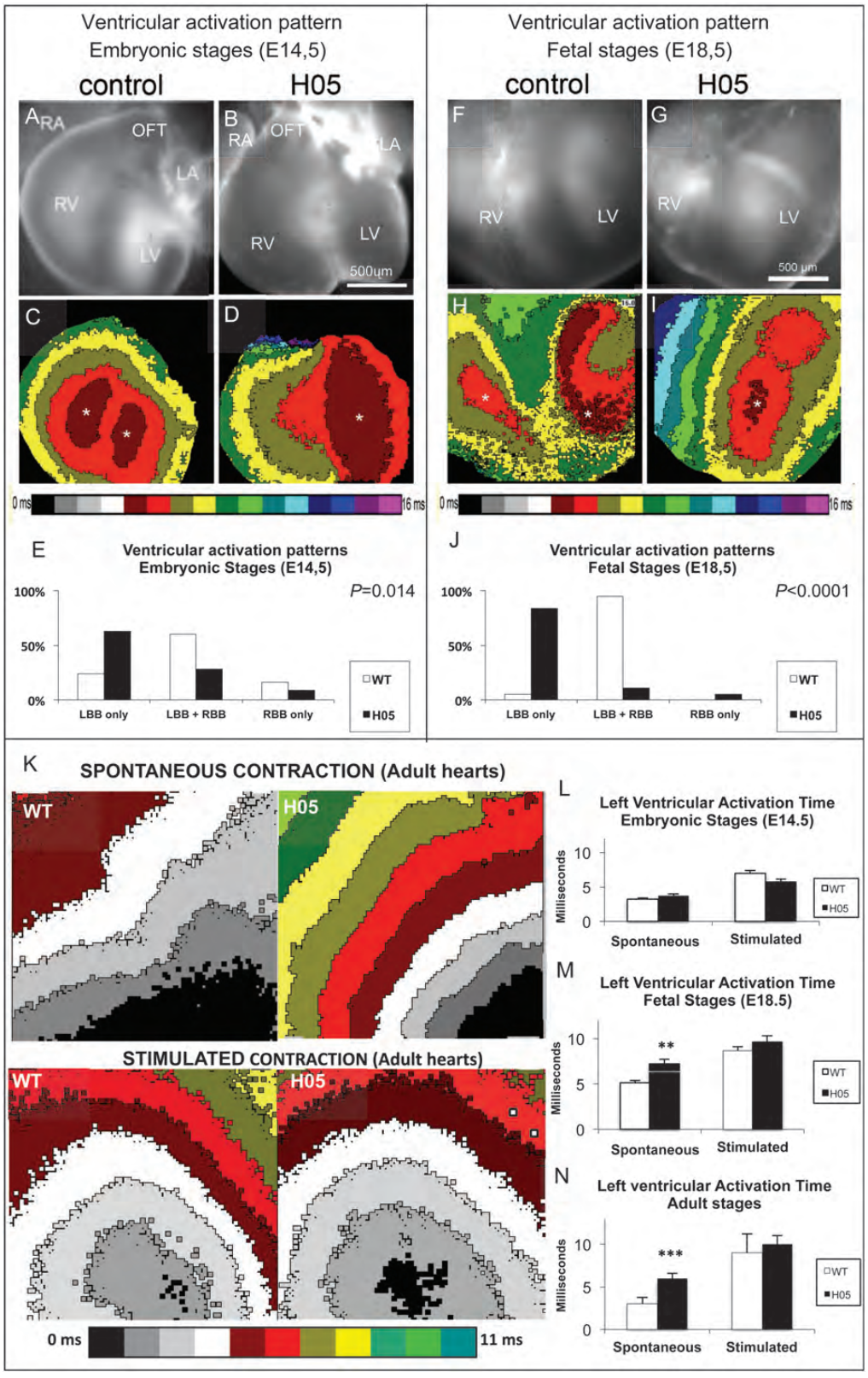


**Figure 4** (*A–E*) Ventricular activation pattern at embryonic stages (E14.5). (*A* and *C*) The first activated region (asterisks) is located in the right and left ventricles in WT and H05 transgenic embryos ($n = 76$ H05 and 76 WT). (*F–J*) Ventricular activation pattern at foetal stages (E18.5). The first activated region turn to be located at the level of the apex in the left ventricle of WT heart (asterisk in H), while H05 foetal hearts maintained left–right ventricular activation (asterisk in I) ($n = 55$ H05 and 55 WT). (*K*) Representative optical maps of adult hearts under spontaneous (superior row) and stimulated (inferior row) contraction ($n = 30$ H05 and 30 WT). (*L–N*) Total left ventricle (LV) activation time at embryonic (E14.5), foetal (E18.5), and adult stages, respectively. ***$P < 0.0001$.

the VCS. The architecture of the adult VCS has been previously described by analysis of GFP fluorescence in *Cx40GFP*$^{/+}$ mice in which the entire VCS can be visualized by GFP reporter gene activity.[12] Three-dimensional visualization and quantification of Cx40+ cell networks by using fluorescent illumination was performed as described previously.[12] GFP expression analysis performed in the H05/Cx40$^{GFP/+}$ transgenic mice at adult stages revealed changes in the ventricular GFP+ cell networks. We found that adult H05/Cx40$^{GFP/+}$ transgenic mice displayed an increase in the number of GFP+ cell networks in the apical portion of the left ventricle, as well as a significant decrease in the number of GFP+ cell networks reaching the left ventricular free wall, when compared with Cx40$^{GFP/+}$ mice (25+1.3 in WT mice vs. 10+1.4 in H05 mice) (*Figure 5A–E*). In addition, analyses of the right ventricle also showed a dramatic decrease in the number of GFP+ cell networks in transgenic hearts compared with WT littermates (40 + 3 in WT vs. 15 + 2 in H05 mice) (*Figure 5 C–F*). Therefore, this analysis revealed the presence of morphological anomalies in the adult VCS of the H05 mouse line.

While a definitive and unequivocal answer about when and how the early VCS is specified remains to be fully elucidated, the ventricular trabeculations have been consistently proposed as a source in particular[18] those expressing Cx40 protein[11] (see Supplementary material online, *Figure S8)*. In this context, Sankova *et al.*[11] have demonstrated that the major ventricular activation patterns correlate with CCS formation in the Cx40$^{GFP/+}$ mouse strain. Furthermore, a recent retrospective clonal analysis in mammalian VCS development using the nlaacZ model into the Cx40$^{GFP/+}$ background has revealed a biphasic mode of VCS development: lineage restriction followed by limited outgrowth.[20] Importantly, these authors have shown that by E16.5 stage of mouse development Cx40$^{GFP}$ expression is restricted to conductive founder cells. Therefore, to investigate whether the morphological alterations in the VCS were developed during the process of cardiogenesis, GFP expression analysis was analysed at foetal (E18.5) and embryonic (E16.5 and E14.5) stages. Our analysis showed that, similar to adults, foetal hearts (E18.5) of the H05/Cx40$^{GFP/+}$ line displayed significant changes in the number of GFP+ cell networks into left (25 + 2 in WT vs. 5 + 1 in H05 mice) and right (30 + 3 in WT vs. 8 + 1 in H05 mice) ventricles (*Figure 5G–K*). Similar results were obtained at E16.5 in which Cx40 expression is already restricted to VCS cell lineage (*Figure 5P–R*). Furthermore, even at E14.5, the number of GFP+ ventricular trabeculations was significantly decreased in H05/Cx40$^{GFP/+}$ mice compared with WT littermates (left ventricle: 30 + 3 in WT vs. 10 + 2 in H05 mice; right ventricle: 23 + 4 in WT mice vs. 5 + 1 in H05 mice) (*Figure 5M–O*). Thus, taken together, these results show that concomitant with early Scn5a and Scn1b upregulation in the VCS during development, this transgenic model of LQTS displays abnormal Cx40$^{GFP}$ patterning which is compatible with morphological abnormalities in the VCS at early cardiac developmental stages.

In order to further explore whether increases in Na+ current lead to the development of VCS morphological abnormalities, we carried out whole embryo cultures experiments in which Cx40$^{GFP/+}$ embryos were exposed to the sodium channel opener anemone toxin ATXII. Due to the limitations of embryo survival in culture, we analysed embryos cultured at +E10.5 stages. It has been previously shown that ATXII increases sodium current and AP durations eliciting polymorphic ventricular tachycardia in mice as well as leading to potentially arrhythmogenic early afterdepolarization in isolated mouse cardiomyocytes.[21] Interestingly and similarly to our findings in H05/Cx40$^{GFP/+}$ transgenic mice, we observed that ATXII-treated embryos exhibited a significant decrease in the number of GFP+ ventricular trabeculations (*Figure 6*), indicating that increased sodium current leads to VCS dysmorphogenesis.

# 4. Discussion

Ion channel impairment is a common finding in the failing heart. Several reports have pointed out that remodelling of ion channel expression secondary to heart rate abnormalities increases the susceptibility to ventricular tachyarrhythmias.[21] Electrical remodelling of the heart occurs in response to both functional (i.e. altered electrical activation) and structural (i.e. heart failure, myocardial infarction, etc.) alterations. Primary electrical remodelling occurs in response to altered patterns of electrical activation without significant structural remodelling, but secondary remodelling arises in response to a structural insult.[22] In this study, we demonstrate that a clear sodium channel upregulation (Scn5a and Scn1b) is already present at embryonic stages in a transgenic model of LQTS. It is interesting to highlight that, while Kv channel expression remodelling begins concomitant with the development of cardiac hypertrophy at the foetal stages (E18.5), sodium channel upregulation is already present in the H05 line at embryonic stages. In this mouse model, overexpression of the dominant-negative isoform of the KvLQT1 potassium channel is under the control of the α-MHC promoter, which is expressed mainly in the atria at early embryonic stages, in the atria, and in different parts of the ventricles at foetal and neonatal stages, and within the entire heart around 1 week after birth.[3] We have detected that overexpression of the dominant-negative isoform of the KvLQT1 is present in the atria as well as in the ventricles of H05 hearts at embryonic stages (E14.5) (see Supplementary material online, *Figure S9*). Thus, we can assume that sodium channel up-regulation occurs after KvLQT1 $K^+$ channel functional inactivation in embryonic H05 hearts and while potassium channel expression remodelling and cardiac hypertrophy are developed later at the foetal stage probably secondary to the arrhythmogenic disorder present in this mouse model of LQTS.

In addition, in this study we provide compelling evidence that functional suppression of the KvLQT1 potassium channel leads to sodium channel upregulation in a transgenic model of LQTS. Furthermore, our *in vitro* and *ex vivo* experiments by using KvLQT1 (Kcnq1) blocker clearly reinforced the notion that KvLQT1 functional suppression elicits sodium channel upregulation. It has been previously demonstrated that calmodulin (CaM) is a constitutive component of KCNQ1 K channel complex.[23] Likewise, previous reports have shown that $Ca^{2+}$/calmodulin-dependent systems mediate rate-dependent ion channel expression remodelling and may enhance $Na^+$ channel membrane expression.[24] The putative involvement of calcineurin/NFAT pathway on sodium channel upregulation in this transgenic model should be further analysed, although it is out of the scope of the present manuscript.

Interestingly, it has been reported that an increase in the $I_{Na}$ density leads to an additional prolongation of the cardiac AP duration, a situation that increases the risk of lethal arrhythmias in the LQTS.[21] Curiously, in transgenic mice overexpressing Scn5a, QRS duration and QTc are normal and the sodium current density as well as the APDs in transgenic ventricular cardiomyocytes are nearly identical to that from non-transgenic cells.[25] However, our patch-clamp analysis revealed that sodium channel upregulation in transgenic ventricular H05 myocytes is associated with an increased peak sodium current

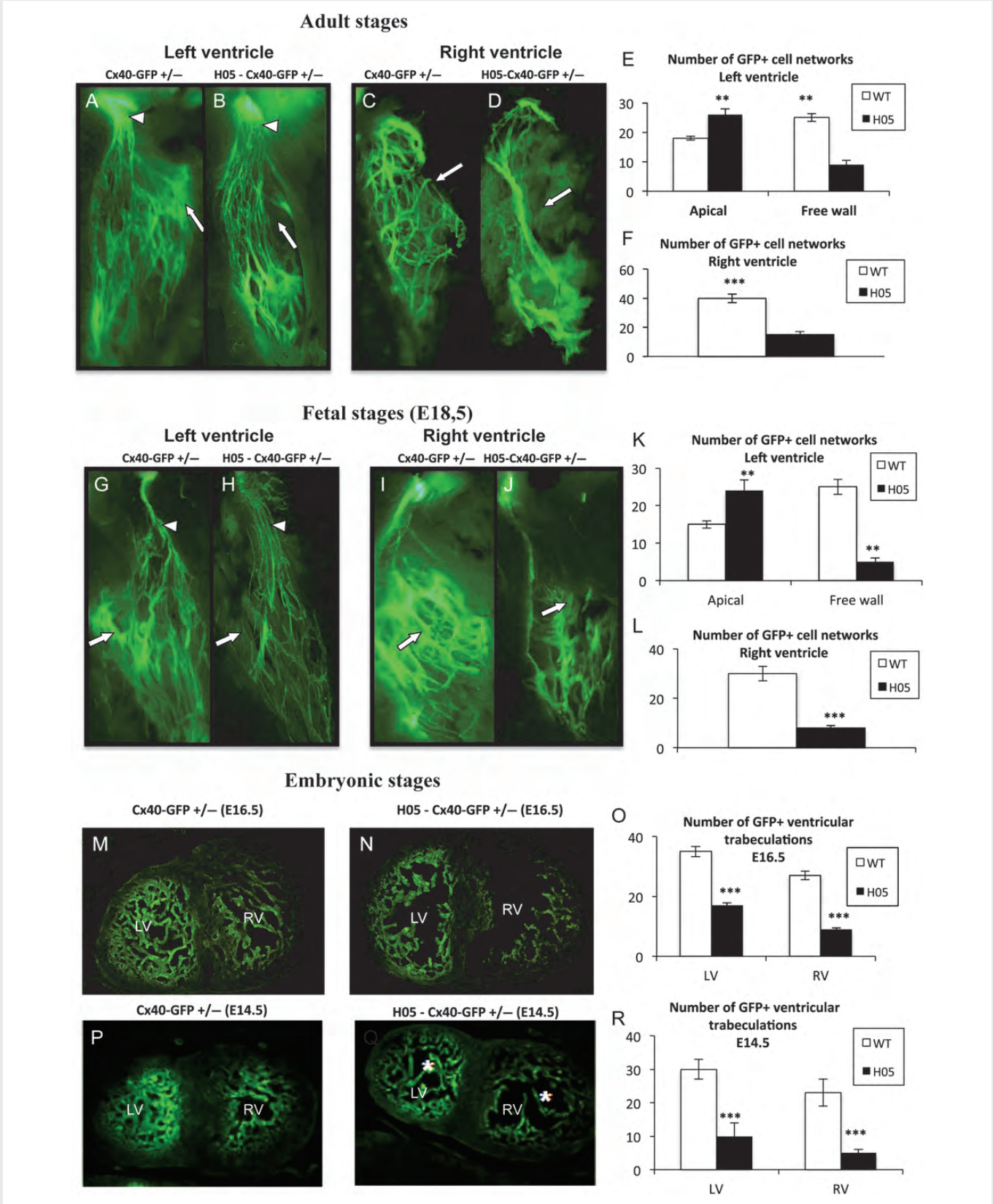


**Figure 5** Architecture of the ventricular conduction system: (*A, B, G, H*) arrowheads: GFP+ cell networks in the apical portion of the left ventricle; arrows: GFP+ cell networks reaching the left ventricular free wall. (*C, D, I, J*) Arrows: GFP+ cell networks in the right ventricle. (*E, F, K, L*) Quantification of GFP+ cell networks at adult ($n = 25$ H05 and 32 WT) and foetal ($n = 40$ H05 and 36 WT) stages, respectively. (*M, N, P, Q*) GFP+ ventricular trabeculations (asterisks) at E16.5 and E14.5 stages, respectively. (*O* and *R*) Quantification of GFP + ventricular trabeculations in the right and left ventricles at E16.5 and E14.5 stages (E14.5: $n = 40$ H05 and 36 WT; E16.5: $n = 32$ H05 and 29 WT). ***$P < 0.001$.

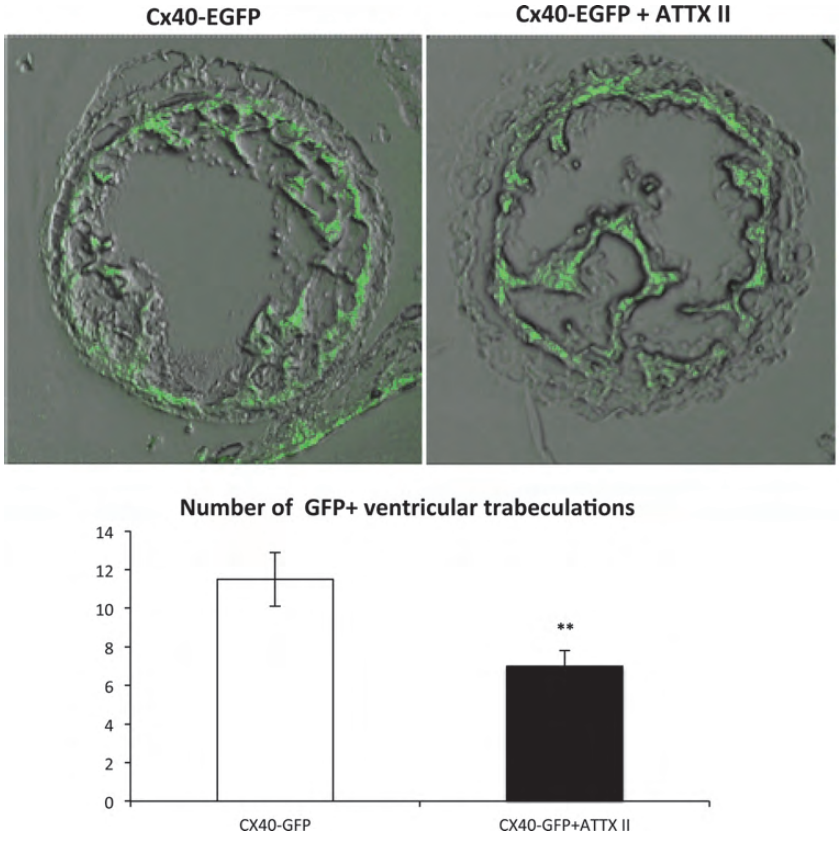


**Figure 6** Cx40GFP embryos treated with ATTX-II. (*A*) Representative image: decrease in the number of GFP+ trabeculations in the primitive left ventricle of Cx40GFP embryos treated compared with control embryos. (*B*) Quantification of number of GFP+ trabeculations in cultured embryos at E10.5 ($n = 15$). $^{**}P < 0.01$.

density, and a delayed recovery of the sodium current from inactivation. Since Scn1b can modulate the sodium current,[15,16] and our transgenic model displays not only Scn5a but also Scn1b upregulation, we cannot rule out that the functional effects of the H05 on the sodium current might be due, at least in part, to β1 subunit upregulation.

It has also been shown that mutations in non-ion channel proteins such as the cytoskeletal protein syntrophin α1 (SNTA1) are associated with LQTS type 3, and these mutations produce Nav1.5 gain of function, as well as increased sodium current density and delayed recovery from sodium channel inactivation.[26] These alterations are similar to the patch-clamp profile found for the H05 mouse line in the present study. Although the full impact of sodium channel remodelling on the electrical configuration of these mice should be further investigated, our findings suggest that sodium channel remodelling may contribute to enhance the arrhythmogenic events.

The VCS represents the 'electrical wiring' responsible for the co-ordination of cardiac contraction. Defects in the circuit produce delay or conduction block and predispose to cardiac arrhythmias. The transfer of electrical impulses from the Purkinje network to the working ventricular myocardium to stimulate ventricular contraction occurs simultaneously from the apex to the base of the heart in a co-ordinated manner. This apex-to-base contraction allows efficient ejection of blood from the ventricles into the outflow tract at the base of the heart.[18] This activation pattern is also present in hearts of lower vertebrates and it is established relatively early during cardiac morphogenesis concomitant with the development of a mature VCS.[18] Our functional analyses by optical mapping of developing hearts of H05 transgenic line revealed developmental delay in the acquisition of the mature pattern of the ventricular activation. Furthermore, total left ventricular activation time was increased when the electrical impulse was conducted through the VCS at foetal and adult stages. This demonstrates that the proper function of the VCS is impaired already in the foetal hearts. Importantly, we found that VCS dysfunction is accompanied by severe changes in its morphology already at early embryonic stages. Thus, to the best of our knowledge, this study demonstrates for the first time the presence of abnormal development of the VCS in an animal model of LQTS.

In addition, we shown that sodium channel upregulation is concomitant to the onset of morphological anomalies in the prospective VCS in H05/Cx40$^{GFP/+}$ embryonic hearts. In this context, it is interesting to highlight that ion current remodelling may have important potential effects on the cardiac Purkinje fibres.[27] In former studies, we have reported that Scn5a and Scn1b are overexpressed in the VCS during developmental stages.[14,16] Moreover, our *ex vivo* analyses provide additional evidence supporting the notion that increases in the peak sodium current lead to VCS malformations. We can speculate that an arrhythmogenic substrate elicited by increased sodium current density leads to a functional overload within VCS and subsequently to a dysmorphogenesis; however, the mechanisms by which

changes in sodium current density lead to CCS dysmorphogenesis require further analyses.

In conclusion, we provide the first direct evidence for a relationship between Kcnq1 dysfunction and early embryonic sodium ion channel remodelling linked to the presence of morphological and functional anomalies in the VCS of the developing heart of a transgenic model of LQTS. These findings provide new insights into the mechanisms underlying foetal and neonatal cardiac electrophysiological disorders, which might help understand how molecular, functional, and morphological alterations are linked to clinical pathologies such as cardiac congenital anomalies, arrhythmias, and perinatal sudden death.

# Supplementary material

Supplementary material is available at *Cardiovascular Research* online.

**Conflict of interest:** none declared.

## Funding

This work was partially supported by grants BFU2012-3811, BFU2009/11566 (Ministerio de Ciencia e Innovación, Gobierno de España), CTS-8053, P08-CTS-3878 (Junta de Andalucia). D.S. was supported by the Ministry of Education VZ 0021620806-PRVOUK-P35/LF1/5, Academy of Sciences Purkinje Fellowship, and institutional AV0Z50110509-RVO:67985823. Further support comes from the Grant Agency of the Czech Republic 304/08/061, P302/11/1308, 204/09/H084, and 13-12412S. B.S. is supported by the Charles University grant for graduate studies.

## References

1. Roberts JD, Gollob MH. The genetic and clinical features of cardiac channelopathies. *Future Cardiol* 2010;**6**:491–506.
2. Scheinman MM. Role of the His-Purkinje system in the genesis of cardiac arrhythmia. *Heart Rhythm* 2009;**6**:1050–1058.
3. Demolombe S, Lande G, Charpentier F, van Roon MA, van den Hoff MJ, Toumaniantz G *et al*. Transgenic mice overexpressing human KvLQT1 dominant-negative isoform. Part I: phenotypic characterisation. *Cardiovasc Res* 2001;**50**:314–327.
4. Dominguez JN, de la Rosa A, Navarro F, Franco D, Aránega AE. Tissue distribution and subcellular localization of the cardiac sodium channel during mouse heart development. *Cardiovasc Res* 2008;**78**:45–52.
5. Chinchilla A, Daimi H, Lozano-Velasco E, Domínguez JN, Caballero R, Delpón E *et al*. PITX2 insufficiency leads to atrial electrical and structural remodeling linked to arrhythmogenesis. *Circ Cardiovasc Genetics* 2011;**4**:269–279.
6. Shimoni Y, Severson D, Giles W. Thyroid status and diabetes modulate regional differences in potassium currents in rat ventricle. *J Physiol* 1995;**488**:673–688.
7. Rapila R, Korhonen T, Tavi P. Excitation-contraction coupling of the mouse embryonic cardiomyocytes. *J Gen Physiol* 2008;**4**:397–405.
8. Seebohm G, Lerche C, Pusch M, Steinmeyer K, Brüggemann A, Busch AE. A kinetic study on the stereospecific inhibition of KCNQ1 and IKs by the chromanol 293B. *Br J Pharmacol* 2001;**134**:1647–1654.
9. Mommersteeg MT, Domínguez JN, Wiese C, Norden J, de Gier-de Vries C, Burch JB *et al*. The sinus venosus progenitors separate and diversify from the first and second heart fields early in development. *Cardiovasc Res* 2010;**87**:92–101.
10. Hewett KW, Norman LW, Sedmera D, Backer RJ, Justus C, Zhang J *et al*. Knockout the neural and the heart expressed gene HF-1b results in apical deficits of ventricular structure and activation. *Cardiovasc Res* 2005;**67**:548–60.
11. Sankova B, Benes J Jr, Jiri B, Krejci E, Dupays L, Theveniau-Ruissy L *et al*. The effect of connexion40 deficiency on ventricular conduction system during development. *Cardiovasc Res* 2012;**95**:469–479.
12. Miquerol L, Meysen S, Mangoni M, Bois P, van Rijen HV, Abran P *et al*. Architectural and functional asymmetry of the His-Purkinje system of the murine heart. *Cardiovasc Res* 2004;**63**:77–86.
13. Moss AJ. Long QT syndrome. *JAMA* 2003;**289**:2041–2044.
14. Cardona K, Trenor B, Rajamani S, Romero L, Ferrero JM, Saiz J. Effects of late sodium current enhancement during LQT-related arrhythmias. A simulation study. *Conf Proc IEEE Eng Med Biol Soc* 2010;**2010**:3237–3240.
15. Mishra S, Undrovinas NA, Maltsev VA, Reznikov V, Sabbah HN, Undrovinas A. Post-transcriptional silencing of SCN1B and SCN2B genes modulates late sodium current in cardiac myocytes from normal dogs and dogs with chronic heart failure. *Am J Physiol Heart Circ Physiol* 2011;**301**:H1596–H1605.
16. Dominguez JN, Navarro F, Franco D, Thompson RP, Aránega AE. Temporal and spatial expression pattern of beta1 sodium channel subunit during heart development. *Cardiovasc Res* 2005;**65**:842–850.
17. Sedmera D, Pexieder T, Vuillemin M, Thompson RP, Anderson RH. Developmental patterning of the myocardium. *Anat Rec* 2000;**258**:319–337.
18. Rentschler S, Vaidya DM, Tamaddon H, Degenhardt K, Sassoon D, Morley GE *et al*. Visualization and functional characterization of the developing murine cardiac conduction system. *Development* 2001;**128**:1785–1792.
19. Vozzi C, Dupont E, Coppen SR, Yeh HI, Severs NJ. Chamber-related differences in connexin expression in the human heart. *J Mol Cell Cardiol* 1999;**31**:991–1003.
20. Miquerol L, Moreno-Rascon N, Beyer S, Dupays L, Meilhac SM, Buckingham ME *et al*. Biphasic development of the mammalian ventricular conduction system. *Circ Res* 2010;**107**:123–13.
21. Lowe JS, Stroud DM, Yang T, Hall L, Atack TC, Roden DM. Increased late sodium current contributes to long QT-related arrhythmia susceptibility in female mice. *Cardiovasc Res* 2012;**95**:300–307.
22. Cutler MJ, Jeyaraj D, Rosenbaum DS. Cardiac electrical remodeling in health and disease. *Trends Pharmacol Sci* 2011;**32**:174–180.
23. Ghosh S, Nunziato DA, Pitt GS. KCNQ1 assembly and function is blocked by Long-QT Syndrome mutations that disrupt interaction with Calmodulin. *Circ Res* 2006;**28**:1048–1054.
24. Dominguez B, Felix R, Monjaraz E. Upregulation of voltage-gated $Na^+$ channels by long-term activation of the ghrelin-growth hormone secretagogue receptor in clonal GC somatotropes. *Am J Physiol Endocrinol Metab* 2009;**296**:E1148–E1156.
25. Zhang T, Yong SL, Tian XL, Wang QK. Cardiac-specific overexpression of SCN5A gene leads to shorter P wave duration and PR interval in transgenic mice. *Biochem Biophys Res Commun* 2007;**355**:444–450.
26. Wu G, Ai T, Kim JJ, Mohapatra B, Xi Y, Li Z *et al*. Alpha-1-syntrophin mutation and the long-QT syndrome: a disease of sodium channel disruption. *Circ Arrhythm Electrophysiol* 2008;**1**:193–201.
27. Han W, Chartier D, Li D, Nattel S. Ionic remodeling of cardiac Purkinje cells by congestive heart failure. *Circulation* 2001;**104**:2095–2100.